Ultrasonic Nanotherapy of Pancreatic Cancer: Lessons from Ultrasound Imaging

Natalya Rapoport,[*,†] Anne M. Kennedy,[‡] Jill E. Shea,[§] Courtney L. Scaife,[§] and Kweon-Ho Nam[†]

Department of Bioengineering, University of Utah, and Departments of Clinical Radiology and Surgery, School of Medicine, University of Utah, Salt Lake City, Utah 84112

Abstract: Pancreatic ductal adenocarcinoma (PDA) is the fourth most common cause of cancer death in the United States, with a median survival time of only 3−6 months for forty percent of patients. Current treatments are ineffective, and new PDA therapies are urgently needed. In this context, ultrasound-mediated chemotherapy by polymeric micelles and/or nanoemulsion/microbubble encapsulated drugs may offer an innovative approach to PDA treatment. PDA xenografts were orthotopically grown in the pancreas tails of nu/nu mice by surgical insertion of red fluorescence protein (RFP)-transfected MiaPaCa-2 cells. Tumor growth was controlled by fluorescence imaging. Occasional sonographic measurements correlated well with the formal tumor tracking by red fluorescence. Tumor accumulation of paclitaxel-loaded nanoemulsion droplets and droplet-to-bubble transition under therapeutic ultrasound was monitored by diagnostic ultrasound imaging. MiaPaCa-2 tumors manifested resistance to treatment by gemcitabine (GEM). This drug is the gold standard for PDA therapy. The GEM-resistant tumors proved sensitive to paclitaxel. Among six experimental groups studied, the strongest therapeutic effect was exerted by the following drug formulation: GEM + nanodroplet-encapsulated paclitaxel (nbGEN) combined with tumor-directed 1-MHz ultrasound that was applied for 30 s four to five hours after the systemic drug injection. Ultrasound-mediated PDA therapy by either micellar or nanoemulsion encapsulated paclitaxel resulted in substantial suppression of metastases and ascites, suggesting ultrasound-enhanced killing of invasive cancerous cells. However, tumors relapsed after the completion of therapy, indicating survival of some tumor cells. The recurrent tumors manifested development of paclitaxel resistance. Ultrasound imaging suggested nonuniform distribution of nanodroplets in the tumor volume due to irregular vascularization, which may result in the development of zones with subtherapeutic drug concentration. This is implicated as a possible cause of the resistance development, which may be pertinent to various modes of tumor nanotherapy.

Keywords: Ultrasound imaging; ultrasound-mediated chemotherapy; pancreatic cancer; paclitaxel; polymeric micelles; nanoemulsions; microbubbles

Introduction

The application of biomedical nanotechnology holds promise for solving major problems in current tumor chemotherapy related to the severe side effects of chemotherapeutic drugs and development of drug resistance. During the past decade, the advances of nanomedicine have allowed for the combination of various functionalities in one molecular or supramolecular construct, i.e. polymeric bioconjugate

---

* Correspondence author. Dr. Natalya Rapoport, Research Professor, Department of Bioengineering, 72 S. Central Campus Dr., Room 2646, University of Utah, Salt Lake City, UT 84112. E-mail: natasha.rapoport@utah.edu. Tel: 1-801-581-8990. Fax: 1-801-585-5361.

† Department of Bioengineering.
‡ Department of Clinical Radiology, School of Medicine.
§ Department of Surgery, School of Medicine.

or nanoparticle. The nanoparticles include polymeric micelles, liposomes, hollow particles, nano- or microemulsion droplets etc. Various chemotherapeutic drugs, imaging agents, and targeting moieties may be encapsulated in the same nanocontainer. This ability to combine chemotherapeutic agents and imaging markers is especially important in oncological practice potentially allowing early assessment of response to treatment.

Among various imaging modalities, ultrasound is the most cost-effective. Ultrasound provides real-time information. The lack of ionizing radiation (in contrast to e.g. CT) is also an advantage. Ultrasound imaging may be combined with ultrasound-mediated drug delivery by ultrasound-responsive nanoparticles. This allows double tumor targeting because nanoparticles accumulate in tumor tissue via the enhanced permeability and retention (EPR) effect,[1] followed by local release of the encapsulated drug in tumor tissue in response to tumor-directed ultrasound.[2−6] These drug nanocarriers are expected to passively accumulate in tumors because of the enhanced permeability and retention (EPR) effect, which is based on defective tumor microvasculature that allows extravasation of drug-loaded nanoparticles through large interendothelial gaps.[7,8] In addition, poor lymphatic drainage of tumors results in longer retention of extravasated particles in tumor tissue. In contrast to tumors, blood vessels in normal tissues have tight interendothelial junctions which do not allow extravasation of nanoparticles.

Effective tumor accumulation of nanoparticles via the EPR effect requires sufficient particle residence time in circulation; to provide for this, nanoparticles are commonly coated with poly(ethylene oxide) chains that suppress blood protein adsorption and prevent particle recognition by the cells of the reticuloendothelial system.

Ultrasound as a drug delivery modality offers a number of important advantages in comparison with other physical modalities. Sonication may be performed noninvasively or minimally invasively through intraluminal, laparoscopic or percutaneous means. For extracorporeal sonication, the transducer is placed in contact with a water-based gel or a water layer on the skin, and no insertion or surgery is required. Ultrasound can be directed toward deeply located body sites, and tumor sonication with millimeter precision is feasible.

During the past decade, a number of groups have concentrated their efforts on developing ultrasound-responsive drug delivery systems for oncological applications.[9−18] Ultrasound as a component of a drug delivery modality may be applied with a variety of drug carriers. Development of ultrasound-responsive stable liposomes that manifested prolonged circulation time and effective tumor targeting was recently reported. Ultrasound-induced heating triggered phase transition in the phospholipid membrane and released the drug in the target region. Ultrasound-triggered delivery of paclitaxel (PTX) to the monolayers of prostate cancer cells from a phospholipid-coated perfluorohexane nanoemulsion developed by ImaRx was also reported.[19]

(1) Iyer, A. K.; Khaled, G.; Fang, J.; Maeda, H. Exploiting the enhanced permeability and retention effect for tumor targeting. *Drug Discovery Today* **2006**, *11* (17−18), 812–8.

(2) Rapoport, N.; Gao, Z.; Kennedy, A. Multifunctional nanoparticles for combining ultrasonic tumor imaging and targeted chemotherapy. *J. Natl. Cancer Inst.* **2007**, *99* (14), 1095–106.

(3) Gao, Z.; Kennedy, A. M.; Christensen, D. A.; Rapoport, N. Y. Drug-loaded nano/microbubbles for combining ultrasonography and targeted chemotherapy. *Ultrasonics* **2008**, *48* (4), 260–70.

(4) Rapoport, N.; Kennedy, A. M.; Shea, J. E.; Scaife, C. L.; Nam, K. H., Controlled and targeted tumor chemotherapy by ultrasound-activated nanoemulsions/microbubbles. *J. Controlled Release*, **2009**, *138*(3): 268–276.

(5) Rapoport, N. Physical stimuli-responsive polymeric micelles for anti-cancer drug delivery. *Prog. Polym. Sci.* **2007**, *32*, 962–90.

(6) Gao, Z. G.; Fain, H. D.; Rapoport, N. Controlled and targeted tumor chemotherapy by micellar-encapsulated drug and ultrasound. *J. Controlled Release* **2005**, *102* (1), 203–22.

(7) Hobbs, S. K.; Monsky, W. L.; Yuan, F.; Roberts, W. G.; Griffith, L.; Torchilin, V. P.; Jain, R. K. Regulation of transport pathways in tumor vessels: role of tumor type and microenvironment. *Proc. Natl. Acad. Sci. U.S.A.* **1998**, *95* (8), 4607–12.

(8) Campbell, R. B. Tumor physiology and delivery of nanopharmaceuticals. *Anticancer Agents Med. Chem.* **2006**, *6* (6), 503–12.

(9) Schroeder, A.; Avnir, Y.; Weisman, S.; Najajreh, Y.; Gabizon, A.; Talmon, Y.; Kost, J.; Barenholz, Y. Controlling liposomal drug release with low frequency ultrasound: mechanism and feasibility. *Langmuir* **2007**, *23* (7), 4019–25.

(10) Schroeder, A.; Honen, R.; Turjeman, K.; Gabizon, A.; Kost, J.; Barenholz, Y., Ultrasound triggered release of cisplatin from liposomes in murine tumors. *J. Controlled Release*, submitted.

(11) Ferrara, K.; Pollard, R.; Borden, M. Ultrasound microbubble contrast agents: fundamentals and application to gene and drug delivery. *Annu. Rev. Biomed. Eng.* **2007**, *9*, 415–47.

(12) Ferrara, K. W. Driving delivery vehicles with ultrasound. *Adv. Drug Delivery Rev.* **2008**, *60* (10), 1097–102.

(13) Unger, E. C.; Porter, T.; Culp, W.; Labell, R.; Matsunaga, T.; Zutshi, R. Therapeutic applications of lipid-coated microbubbles. *Adv. Drug Delivery Rev.* **2004**, *56* (9), 1291–314.

(14) Wheatley, M. A.; Forsberg, F.; Oum, K.; Ro, R.; El-Sherif, D. Comparison of in vitro and in vivo acoustic response of a novel 50:50 PLGA contrast agent. *Ultrasonics* **2006**, *44* (4), 360–7.

(15) Qin, S.; Caskey, C. F.; Ferrara, K. W. Ultrasound contrast microbubbles in imaging and therapy: physical principles and engineering. *Phys. Med. Biol.* **2009**, *54* (6), R27–57.

(16) Zheng, H.; Kruse, D. E.; Stephens, D. N.; Ferrara, K. W.; Sutcliffe, P.; Gardner, E. A sensitive ultrasonic imaging method for targeted contrast microbubble detection. *Conf. Proc. IEEE Eng. Med. Biol. Soc.* **2008**, *2008*, 5290–3.

(17) Kheirolomoom, A.; Dayton, P. A.; Lum, A. F.; Little, E.; Paoli, E. E.; Zheng, H.; Ferrara, K. W. Acoustically-active microbubbles conjugated to liposomes: characterization of a proposed drug delivery vehicle. *J. Controlled Release* **2007**, *118* (3), 275–84.

(18) Borden, M. A.; Kruse, D. E.; Caskey, C. F.; Zhao, S.; Dayton, P. A.; Ferrara, K. W. Influence of lipid shell physicochemical properties on ultrasound-induced microbubble destruction. *IEEE Trans. Ultrason. Ferroelectr. Freq. Control* **2005**, *52* (11), 1992–2002.

(19) Dayton, P. A.; Zhao, S.; Bloch, S. H.; Schumann, P.; Penrose, K.; Matsunaga, T. O.; Zutshi, R.; Doinikov, A.; Ferrara, K. W. Application of ultrasound to selectively localize nanodroplets for targeted imaging and therapy. *Mol. Imaging* **2006**, *5* (3), 160–74.

Polymeric micelles that combined passive tumor-targeting ability with ultrasound responsiveness were suggested in earlier works of Rapoport's group.[2,6,20−25] It was demonstrated that drug-loaded polymeric micelles accumulated passively in tumor tissue.[26] Ultrasonic irradiation of the tumor enhanced micelle uptake triggered drug release from the micelles and transiently altered cell membrane permeability, resulting in effective intracellular drug internalization by tumor cells. Ultrasound irradiation also enhanced drug diffusion throughout tumor volume, thus reducing drug concentration gradients.[2,6,26] Substantial reduction of the tumor growth rate was achieved using this drug delivery modality.[6,27]

All therapeutic modalities associated with application of physical stimuli, such as tumor ablation induced by radiofrequency, microwave, or ultrasound as well as local mild hyperthermia, require imaging of targeted sites prior to and during treatment. Though various imaging modalities may be used, combining ultrasound-mediated drug delivery with ultrasound imaging appears especially attractive by virtue of offering real time information, versatility, and cost effectiveness. In this context, during the past decade, microbubbles have attracted attention as drug carriers and enhancers of drug and gene delivery. In current clinical practice, microbubbles have been used as ultrasound contrast agents for cardiovascular imaging.[28] Several research groups have concentrated their efforts on developing microbubble-based drug delivery systems.[2,3,11−13,15,16,19,29−42]

The most cost-effective way to solve this problem would be to impart drug carrier properties to FDA approved ultrasound contrast agents such as Optison (Amersham Inc.) or Definity (Lanteus Medical Imaging Inc.). However, currently used contrast agents present a number of inherent problems as drug carriers. Their very short circulation time (minutes) and relatively large size (two to ten micrometers) do not allow effective extravasation into tumor tissue, which is an essential prerequisite for effective drug targeting.

(20) Husseini, G. A.; Myrup, G. D.; Pitt, W. G.; Christensen, D. A.; Rapoport, N. Y. Factors affecting acoustically triggered release of drugs from polymeric micelles. *J. Controlled Release* **2000**, *69* (1), 43–52.

(21) Rapoport, N.; Marin, A.; Christensen, D. A. Ultrasound-activated micellar drug delivery. *Drug Delivery Syst. Sci.* **2002**, *2* (2), 37–46.

(22) Rapoport, N. Factors affecting ultrasound interactions with polymeric micelles and viable cells. In *Carrier-based drug delivery*; Swenson, S., Ed.; ACS Symposium Series; American Chemical Society: Washington, DC, 2004; pp 161−73.

(23) Rapoport, N. Combined cancer therapy by micellar-encapsulated drug and ultrasound. In *Nanotechnology for cancer therapy*; Amiji, M., Ed.; CRC Press: Boca Raton, FL, 2006; pp 417−37.

(24) Rapoport, N. Tumor targeting by polymeric assemblies and ultrasound activation. In *MML*; Arshadi, R., Kono, K., Eds.; Kentus Books: London, U.K., 2006; Vol. 8, pp 305−62.

(25) Kamaev, P.; Rapoport, N. Effect of anticancer drug on the cell sensitivity to ultrasound in vitro and in vivo. *Am. Inst. Phys. Conf. Proc.* **2006**, *829* (1), 543–7.

(26) Gao, Z.; Fain, H. D.; Rapoport, N. Ultrasound-enhanced tumor targeting of polymeric micellar drug carriers. *Mol. Pharmaceutics* **2004**, *1* (4), 317–30.

(27) Howard, B.; Gao, Z.; Lee, S. W.; Seo, M. H.; Rapoport, N. Ultrasound-enhanced chemotherapy of drug-resistant breast cancer tumors by micellar-encapsulated paclitaxel. *Am. J. Drug Delivery* **2006**, *4* (2), 97–104.

(28) Becher, H.; Lofiego, C.; Mitchell, A.; Timperley, J. Current indications for contrast echocardiography imaging. *Eur. J. Echocardiogr.* **2005**, *6*, S1–5.

(29) Greenleaf, W. J.; Bolander, M. E.; Sarkar, G.; Goldring, M. B.; Greenleaf, J. F. Artificial cavitation nuclei significantly enhance acoustically induced cell transfection. *Ultrasound Med. Biol.* **1998**, *24* (4), 587–95.

(30) Kost, J.; Mitragotri, S.; Gabbay, R. A.; Pishko, M.; Langer, R. Transdermal monitoring of glucose and other analytes using ultrasound. *Nat. Med.* **2000**, *6* (3), 347–50.

(31) Taniyama, Y.; Tachibana, K.; Hiraoka, K.; Namba, T.; Yamasaki, K.; Hashiya, N.; Aoki, M.; Ogihara, T.; Yasufumi, K.; Morishita, R. Local delivery of plasmid DNA into rat carotid artery using ultrasound. *Circulation* **2002**, *105* (10), 1233–9.

(32) Unger, E. C.; Hersh, E.; Vannan, M.; McCreery, T. Gene delivery using ultrasound contrast agents. *Echocardiography* **2001**, *18* (4), 355–61.

(33) Mitragotri, S. Healing sound: the use of ultrasound in drug delivery and other therapeutic applications. *Nat. Rev. Drug Discovery* **2005**, *4* (3), 255–60.

(34) Sheikov, N.; McDannold, N.; Sharma, S.; Hynynen, K. Effect of focused ultrasound applied with an ultrasound contrast agent on the tight junctional integrity of the brain microvascular endothelium. *Ultrasound Med. Biol.* **2008**, *34* (7), 1093–104.

(35) Hynynen, K. Ultrasound for drug and gene delivery to the brain. *Adv. Drug Delivery Rev.* **2008**, *60* (10), 1209–17.

(36) McDannold, N.; Vykhodtseva, N.; Hynynen, K. Effects of acoustic parameters and ultrasound contrast agent dose on focused-ultrasound induced blood-brain barrier disruption. *Ultrasound Med. Biol.* **2008**, *34* (6), 930–7.

(37) Shaw, G. J.; Meunier, J. M.; Huang, S. L.; Lindsell, C. J.; McPherson, D. D.; Holland, C. K., Ultrasound-enhanced thrombolysis with tPA-loaded echogenic liposomes. *Thromb. Res.*, submitted.

(38) Kopechek, J. A.; Abruzzo, T. M.; Wang, B.; Chrzanowski, S. M.; Smith, D. A.; Kee, P. H.; Huang, S.; Collier, J. H.; McPherson, D. D.; Holland, C. K. Ultrasound-mediated release of hydrophilic and lipophilic agents from echogenic liposomes. *J. Ultrasound Med.* **2008**, *27* (11), 1597–606.

(39) Smith, D. A.; Porter, T. M.; Martinez, J.; Huang, S.; MacDonald, R. C.; McPherson, D. D.; Holland, C. K. Destruction thresholds of echogenic liposomes with clinical diagnostic ultrasound. *Ultrasound Med. Biol.* **2007**, *33* (5), 797–809.

(40) Datta, S.; Coussios, C. C.; Ammi, A. Y.; Mast, T. D.; de Courten-Myers, G. M.; Holland, C. K. Ultrasound-enhanced thrombolysis using Definity as a cavitation nucleation agent. *Ultrasound Med. Biol.* **2008**, *34* (9), 1421–33.

(41) Miller, D. L.; Averkiou, M. A.; Brayman, A. A.; Everbach, E. C.; Holland, C. K.; Wible, J. H., Jr.; Wu, J. Bioeffects considerations for diagnostic ultrasound contrast agents. *J Ultrasound Med.* **2008**, *27* (4), 611–32; quiz 633−6.

(42) Tartis, M. S.; Kruse, D. E.; Zheng, H.; Zhang, H.; Kheirolomoom, A.; Marik, J.; Ferrara, K. W. Dynamic microPET imaging of ultrasound contrast agents and lipid delivery. *J. Controlled Release* **2008**, *131* (3), 160–6.

A possible way to solve the above problem may consist in developing drug-loaded, nanoscaled microbubble precursors that would effectively accumulate in tumor tissue and then convert into microbubbles in situ after tumor accumulation. With this in mind, we have recently developed block copolymer stabilized echogenic (i.e., ultrasound contrast generating) perfluoropentane (PFP) nanoemulsions that convert into microbubbles under ultrasound irradiation.[2,3,43,44] The nanoemulsions are produced from drug-loaded poly-(ethylene oxide)-*co*-poly(L-lactide) (PEG-PLLA) or poly-(ethylene oxide-*co*-polycaprolactone) (PEG-PCL) micelles by introducing a phase-shift perfluorocarbon compound, perfluoropentane (PFP). The PFP has a boiling temperature of 29 °C. However, PFP nanoemulsions manifest remarkable thermal stability due to the excessive pressure called Laplace pressure inside nanodroplets.[4,43] The thermal stability of PFP nanoemulsions prevents their conversion into microbubbles in circulation. They maintain their nanoscale size, which allows tumor accumulation by extravasation through leaky tumor microvasculature (i.e., passive targeting).[2,4] Without ultrasound, the drug is tightly retained inside the droplet walls, which is important for effective tumor targeting.[4] After tumor accumulation, droplet-to-bubble conversion is triggered by tumor-directed ultrasound. This effect is called acoustic droplet vaporization (ADV).[45] Tumor irradiation by therapeutic ultrasound induces localized drug release from nanodroplets and microbubbles and effective intracellular drug uptake by tumor cells, which in turn, results in effective tumor regression. In addition, primary small microbubbles coalesce into larger microbubbles and provide a long-lasting ultrasonic contrast.[2–4] Using this treatment modality, effective tumor regression was observed in mouse models of breast and ovarian cancer[2–4] the first promising results for pancreatic cancer were presented in ref 4.

Pancreatic ductal adenocarcinoma (PDA) is the fourth most common cause of cancer death in the United States. As noted in ref 46, "The annual incidence rate of pancreatic cancer is almost identical to the mortality rate; approximately 37,000 new cases are diagnosed each year in the United States, and approximately 33,000 patients die from this disease." Only 4% of patients are alive 5 years after the time of diagnosis. Most PDA presentations are inoperable at the time of diagnosis due to the extensive tumor burden, local invasion, poor general health, and multiple aggressive micrometastases that are resistant to chemotherapy and radiation treatment. About 40% of patients have a dismal prognosis; median survival time is only 3−6 months.[46]

The only FDA-approved chemotherapeutic agent for PDA is a nucleoside analogue gemcitabine (GEM), but the partial response rate to chemotherapy is well below 10%[47,48] most probably due to the development of GEM resistance in the course of chemotherapy. Despite low effectiveness, GEM remains the cornerstone of neoadjuvant and adjuvant chemotherapy in pancreatic cancer and imparts a progression-free survival interval ranging from 0.9 to 4.2 months.[49] Neither biotherapies based on the targeted gene therapy, use of antibodies against vascular endothelial growth factor (VEGF) or epithelial growth factor (EGF-R) receptors[50] nor high-intensity ultrasonic tumor ablation[51−54] proved successful. An attempt was made to treat pancreatic cancer by extracorporeal high intensity focused ultrasound (HIFU), with only marginal success.[55]

New approaches to PDA treatment are urgently needed. In this context, ultrasound-mediated chemotherapy by poly-

(43) Rapoport, N.; Efros, A. L.; Christensen, D. A.; Kennedy, A. M.; Nam, K. H., Microbubble generation in phase-shift nanoemulsions used as anticancer drug carriers. *Bubble Sci., Eng. Technol.*, **2009**, *1*(1/2), 31–39.

(44) Nam, K. H.; Christensen, D. A.; Kennedy, A. M.; Rapoport, N. Acoustic droplet vaporization, cavitation, and therapeutic properties of copolymer-stabilized perfluorocarbon nanoemulsions. *Am. Inst. Phys. Conf. Proc.* **2009**, *1113* (1), 124–8.

(45) Kripfgans, O. D.; Fowlkes, J. B.; Miller, D. L.; Eldevik, O. P.; Carson, P. L. Acoustic droplet vaporization for therapeutic and diagnostic applications. *Ultrasound Med. Biol.* **2000**, *26* (7), 1177–89.

(46) Saif, M. W. New developments in the treatment of pancreatic cancer. Highlights from the "44th ASCO Annual Meeting". Chicago, IL, USA. May 30−June 3, 2008. *JOP* **2008**, *9*, (4), 391−7.

(47) Ducreux, M.; Rougier, P.; Fandi, A.; Clavero-Fabri, M. C.; Villing, A. L.; Fassone, F.; Fandi, L.; Zarba, J.; Armand, J. P. Effective treatment of advanced biliary tract carcinoma using 5-fluorouracil continuous infusion with cisplatin. *Ann. Oncol.* **1998**, *9* (6), 653–6.

(48) Burris, H. A., 3rd; Moore, M. J.; Andersen, J.; Green, M. R.; Rothenberg, M. L.; Modiano, M. R.; Cripps, M. C.; Portenoy, R. K.; Storniolo, A. M.; Tarassoff, P.; Nelson, R.; Dorr, F. A.; Stephens, C. D.; Von Hoff, D. D. Improvements in survival and clinical benefit with gemcitabine as first-line therapy for patients with advanced pancreas cancer: a randomized trial. *J. Clin. Oncol.* **1997**, *15* (6), 2403–13.

(49) Moore, M. J.; Hamm, J.; Dancey, J.; Eisenberg, P. D.; Dagenais, M.; Fields, A.; Hagan, K.; Greenberg, B.; Colwell, B.; Zee, B.; Tu, D.; Ottaway, J.; Humphrey, R.; Seymour, L. Comparison of gemcitabine versus the matrix metalloproteinase inhibitor BAY 12−9566 in patients with advanced or metastatic adenocarcinoma of the pancreas: a phase III trial of the National Cancer Institute of Canada Clinical Trials Group. *J. Clin. Oncol.* **2003**, *21* (17), 3296–302.

(50) Tamada, K.; Wang, X. P.; Brunicardi, F. C. Molecular targeting of pancreatic disorders. *World J. Surg.* **2005**, *29* (3), 325–33.

(51) Melodelima, D.; Lafon, C.; Prat, F.; Theillere, Y.; Arefiev, A.; Cathignol, D. Transoesophageal ultrasound applicator for sector-based thermal ablation: first in vivo experiments. *Ultrasound Med. Biol.* **2003**, *29* (2), 285–91.

(52) Prat, F.; Lafon, C.; De Lima, D. M.; Theilliere, Y.; Fritsch, J.; Pelletier, G.; Buffet, C.; Cathignol, D. Endoscopic treatment of cholangiocarcinoma and carcinoma of the duodenal papilla by intraductal high-intensity US: Results of a pilot study. *Gastrointest. Endosc.* **2002**, *56* (6), 909–15.

(53) Prat, F.; Lafon, C.; Margonari, J.; Gorry, F.; Theillere, Y.; Chapelon, J. Y.; Cathignol, D. A high-intensity US probe designed for intraductal tumor destruction: experimental results. *Gastrointest. Endosc.* **1999**, *50* (3), 388–92.

(54) Prat, F.; Lafon, C.; Theilliere, J. Y.; Fritsch, J.; Choury, A. D.; Lorand, I.; Cathignol, D. Destruction of a bile duct carcinoma by intraductal high intensity ultrasound during ERCP. *Gastrointest. Endosc.* **2001**, *53* (7), 797–800.

meric micelles and/or nanoemulsion/microbubble encapsulated drugs may offer an innovative approach to PDA treatment. Important physical properties of PFP nanoemulsions allow drug encapsulation, tumor-targeting, enhanced intracellular drug delivery, and enhanced tumor visibility. The success of our pilot studies[4] suggests that drug delivery in PFP nanoemulsions combined with noninvasive or minimally invasive ultrasound-mediated chemotherapy may allow development of curative rather than palliative therapy for pancreatic cancer. Here we present and discuss advantages and limitations of this approach for therapy and imaging of human MiaPaCa-2 pancreatic cancer xenografts inoculated in nu/nu mice. Cancer cells were transfected with red fluorescent protein (RFP) to allow comparison of RFP and ultrasound imaging data.

Materials and Methods

Block Copolymer. Block copolymers used in this study were bought from Polymer Source Inc. (Montreal, Quebec, Canada). The PEG-PLLA copolymer had a total molecular weight of 9,700; the molecular weights of a hydrophilic PEG block and a hydrophobic PLLA block were 5,000 Da and 4,700 Da respectively, and the number of the monomer units in the corresponding blocks was 113.6 and 54.7.

Micellar Solutions and Drug Loading. Micellar solutions of the PEG-PLLA and PEG-PCL block copolymers were prepared by a solvent exchange technique as described in detail previously.[2] Genexol-PM (GEN) was obtained from Samyang Corp. (Daejeon, South Korea). Genexol PM is a powder formulation that contains 100 mg of PTX in 850 mg of Genexol PM powder (other components are mPEG-PLA and lactose). A desired weight of the GEN powder was dissolved either in PBS or in the PEG-PLLA micellar solution; this composition is designated mGEN.

Formulations. Paclitaxel-loaded PFP nanoemulsions (nb-GEN) were prepared as follows: 1 vol % PFP was added to mGEN, and samples were sonicated in ice-cold water by 20 kHz ultrasound until all PFP was transferred into an emulsion. GEM was added to this composition in a desired concentration.

Particle Size Distribution. Size distribution of nanoparticles was measured by dynamic light scattering at a scattering angle of 165° using a Delsa Nano S instrument (Beckman Coulter, Osaka, Japan) equipped with a 658 nm laser and a temperature controller. Particle size distribution was analyzed using the non-negative least squares (NNLS) method.

Sonication. Unfocused 1 MHz ultrasound was generated by an Omnisound 3000 instrument (Accelerated Care Plus Inc., Sparks, NV). Pressure generated by the transducer was measured with an ONDA needle hydrophone (Onda HNR-

0500). Mechanical index (MI) was calculated according to the equation $MI = P_{r.3}/F^{0.5}$, where peak rarefactional pressure $P_r = 0.61$ MPa and $F = 1$ MHz. In our experiments, MI = 0.59 was used.

Cells. Pancreatic cancer MiaPaCa-2 cells were obtained from American Type Culture Collection (Manassas, VA). Cells were maintained in DMEM supplemented with 10% heat-inactivated fetal bovine serum (FBS). MiaPaCa-2 cells were transfected with red fluorescence protein (RFP) according to the procedure described in refs 56, 57. Cells were cultured at 37 °C in humidified air containing 5% CO_2.

Animal Procedures. Orthotopic pancreatic cancer was inoculated surgically in the pancreatic tail.[57] Mice received a single subcapsular injection of 106 red fluorescent protein labeled MiaPaCa-2 cells suspended in 0.125 mL of serum free media (DMEM). All procedures were done utilizing a 12X Universal S3B microscope (Carl Zeiss, Thornwood, NY).

Following the primary surgery, high resolution (3456 pixels × 2304 pixels) whole body digital images (EOS Digital Rebel, Canon USA, Lake Success, NY) of each mouse were obtained once a week to monitor primary tumor growth and presence of metastases. The red fluorescent protein was visualized with an Illumatool Bright Light System that consisted of a 563 nm excitation filter and a 587 nm emission filter (model LT-9900, LightTools Research, Encinitas, CA). Animals were imaged under nose-cone induced isoflurane general anesthesia. Primary tumor area was quantified using public domain software ImageJ (National Institutes of Health http://rsb.info.nih.gov/ij/).

Animals were randomly assigned to six groups, six animals each: (1) negative control (injection of PBS); (2) GEM at 140 mg/kg (positive control 1); (3) GEN at 20 mg/kg as PTX (positive control 2); (4) GEM + GEN combination treatment; (5) GEN + ultrasound; (6) GEM + nbGEN + ultrasound. Unfocused continuous wave 1 MHz ultrasound was applied extracorporeally for 30 s to the pancreas region of the abdomen. Nominal ultrasound intensity was 3.4 W/cm^2, which corresponded to a measured MI = 0.59. Ultrasound was applied extracorporeally to the abdominal area in the pancreas region through a water bag coupled from both sides to ultrasound transducer and mouse skin by the ultrasound coupling gel. Ultrasound was applied 4 to 5 h after drug injection. In the first treatment round, drug was injected twice a week for two weeks, then there was a break for two weeks, and the treatment was repeated using the same protocol as in the first treatment round. The dose of PTX was the same in all formulations used in this study.

(55) Wu, F.; Wang, Z. B.; Zhu, H.; Chen, W. Z.; Zou, J. Z.; Bai, J.; Li, K. Q.; Jin, C. B.; Xie, F. L.; Su, H. B. Feasibility of US-guided high-intensity focused ultrasound treatment in patients with advanced pancreatic cancer: initial experience. *Radiology* **2005**, *236* (3), 1034–40.

(56) Scaife, C. L.; Shea, J. E.; Dai, Q.; Firpo, M. A.; Prestwich, G. D.; Mulvihill, S. J. Synthetic extracellular matrix enhances tumor growth and metastasis in an orthotopic mouse model of pancreatic adenocarcinoma. *J. Gastrointest. Surg.* **2008**, *12* (6), 1074–80.

(57) Torgenson, M. J.; Shea, J. E.; Firpo, M. A.; Dai, Q.; Mulvihill, S. J.; Scaife, C. L. Natural history of pancreatic cancer recurrence following "curative" resection in athymic mice. *J. Surg. Res.* **2008**, *149* (1), 57–61.
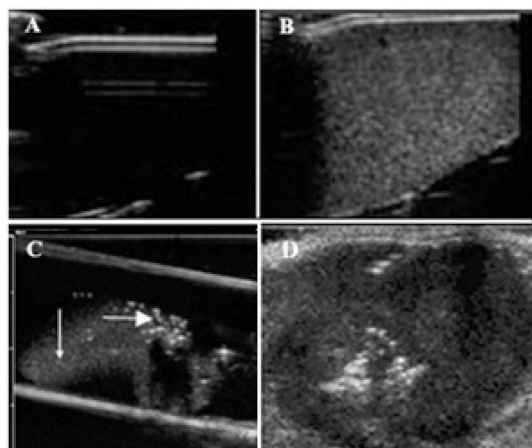
Figure 1. Ultrasound images of nanodroplets/microbubbles; (A) water in a test tube; (B) PFP/PEG-PCL nanodroplets in a test tubes, (C) PFP/PEG-PCL nanodroplets injected into agarose gel through a 26 G needle; (D) PFP/PEG-PCL nanodroplets injected into a subcutaneous pancreatic tumor through a 26 G needle.

In Vivo Ultrasound Imaging. Ultrasound imaging was performed using a 14 MHz linear transducer (Acuson Sequoia 512, Siemens, Mountain View, CA).

Results

Nanoparticle Size Distributions in Initial Formulations. The size distribution parameters for PEG-PLLA micelles and nanodroplets at room temperature are presented in Table 1 in the Supporting Information (adapted from ref 4). The size distribution of micelles was bimodal, with smaller particles corresponding presumably to individual spherical micelles while larger particles represent either wormlike micelles or micellar aggregates. For both types of particles, paclitaxel-loaded micelles (29.3 nm) were larger than empty micelles (22.2 nm). The formation of a nanoemulsion after perfluoropentane (PFP) introduction resulted in the disappearance of small micelles and generation of nanodroplets (592.6 nm, 73%). For paclitaxel-loaded systems, introduction of PFP resulted in a trimodal size distribution. The size of micelles dropped from 29.3 to 19.3 nm while the size of nanodroplets increased from 592.6 to 718.4 nm, suggesting paclitaxel transfer from micelles to nanodroplets. Based on this information, in the formulation used in vivo, the entirety of the drug may be considered located in nanodroplets.

Echogenicity of Nanodroplets and Microbubbles. Due to a large difference between acoustic impedance of PFP nanodroplets or microbubbles and water or biological tissues, both PFP nanodroplets and microbubbles manifest echogenic properties (i.e., ultrasound backscattering) thus developing ultrasound contrast (Figure 1A−C). However, contrast enhancement by microbubbles is much stronger than that by nanodroplets (compare brightness of bubbles indicated by horizontal arrow in Figure 1C with that of droplets indicated by vertical arrow in Figure 1C). This feature allows discrimination between droplets and bubbles after in vivo
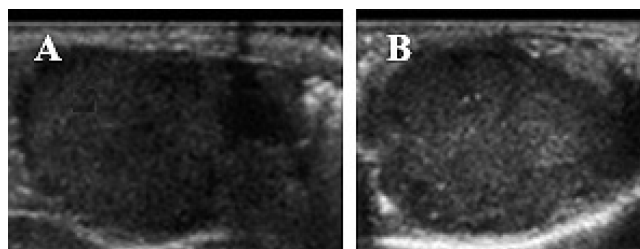
Figure 2. Ultrasound images of the orthotopic pancreatic tumor (A) immediately after and (B) one day after systemic injection of paclitaxel-loaded PFP/PEG-PLLA (nbGEN) nanoemulsion. The increase in grayscale (from 34 to 58 arbitrary units as measured by Image J software) manifests tumor accumulation of nanodroplets.

injections. When PFP nanoemulsions are injected directly into the tumor, a very strong and long-lasting ultrasound contrast is generated due to a partial droplet-to-bubble conversion and bubble coalescence (Figure 1D).[2,43] The grayscale intensity of tumors also increases after systemic injections of nanoemulsions, indicating nanodroplet extravasation into tumor tissue,[4] though this effect is not as strong and punctate as after direct intratumoral injections (Figure 2, compare gray scale before (A) and after injection of paclitaxel (PAX)-loaded PFP/PEG-PLLA nanoemulsion (B).

Tumor sonication after nanodroplet accumulation results in an increase in brightness of bright specks that have been already present in the selected tumor slice; formation of new bright specks is visible in their vicinity (compare the sites indicated by arrows in Figure 3, panels A, B). This suggests ultrasound-induced, highly localized droplet-to-bubble conversion in tumor tissue in the vicinity of pre-existing microbubbles, as was earlier observed in model experiments on microbubbles inserted in the agarose gel or plasma clot.[4,43] Though it is difficult to image exactly the same plane at different days, it appears that bright specks are gradually spreading into the lines with slightly increased brightness (Figure 3C). The data presented above suggest that drug-loaded PFP nanodroplets accumulate in the pancreatic tumor tissue after systemic injection and can be converted into microbubbles under the ultrasound action, which is the foundation of the chemotherapeutic modality presented below.

Pancreatic MiaPaCa-2 Tumors Are Resistant to Gemcitabine but Sensitive to Paclitaxel. Tumor growth curves for animals treated by gemcitabine (GEM), micellar formulation of paclitaxel Genexol PM (GEN), combination drug Genexol PM + GEM, and nanoemulsion formulation of paclitaxel nbGEN + GEM and ultrasound are presented in Figure 4. Good correlation was observed between tumor sizes measured by RFP and ultrasound imaging. GEM-treated tumors grew with the same rate as control while those treated with PTX-containing formulations dramatically regressed, indicating sensitivity to PTX.

Ultrasound-Mediated Chemotherapy of Pancreatic Cancer. As shown in Figure 4, systemic chemotherapy by nanodroplet encapsulated paclitaxel combined with GEM and

Figure 3. Effect of 1 min tumor sonication by 90 kHz ultrasound on the droplet-to-bubble conversion in tumor tissue. Formation of microbubbles is manifested by increased brightness of the pre-existing bright specks visible in panel A and formation of new bright specks (compare panels A and B; specks of interest are indicated by arrows). With time, highly localized bright specks disappear leaving behind lines with a slightly increased brightness (C); K, kidney.
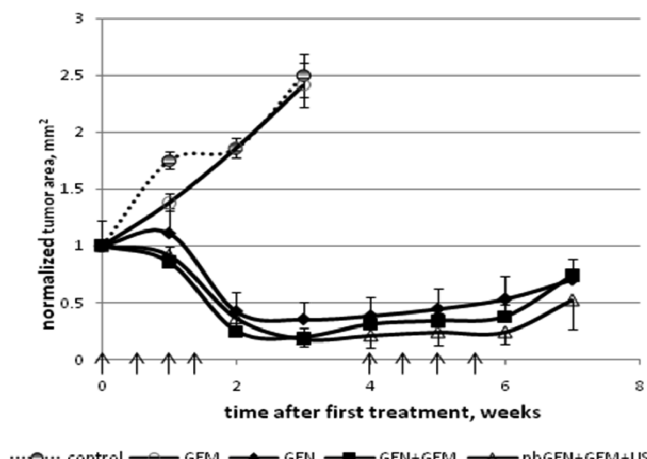

Figure 4. Pancreatic tumor growth curves. Dotted line: control group. Animals were treated by gemcitabine (GEM) (closed circles), micellar encapsulated paclitaxel Genexol PM (GEN) (closed diamonds), combination drug GEM + Genexol PM (closed squares), and combination drug GEM + nanodroplet encapsulated paclitaxel nbGEN combined with continuous wave 1 MHz ultrasound applied for 30 s at 3.4 W/cm^2 nominal power density to the mouse abdominal area in the pancreas region (open triangles). Mean tumor projection areas ± standard error are presented ($N = 6$). Arrows indicate days of treatment. Adapted with modification from ref 4, with permission from Elsevier.

ultrasound resulted in dramatic tumor regression. The gemcitabine that was added in this formulation has a very high aqueous solubility, is not internalized by either micelles or droplets and circulates independently.

The effect of the combined treatment with nanodroplet encapsulated Genexol PM, GEM and ultrasound was the strongest among the six treatment protocols reported in the experimental section (for instance, $P \ll 0.001$ for GEM + nbGEN + ultrasound vs Genexol PM treatment in a paired t test) (Figure 4). The ultrasound effect on the treatment by the nanodroplet encapsulated paclitaxel (nbGEN) was stronger than that on micellar encapsulated paclitaxel (Genexol PM).[4] Even a very large initial tumor effectively regressed under the combined action of nanodroplet encapsulated paclitaxel and ultrasound (Figure 5). Interestingly, the treatments that involved tumor sonication resulted in a significantly reduced number of metastatic foci and suppres-
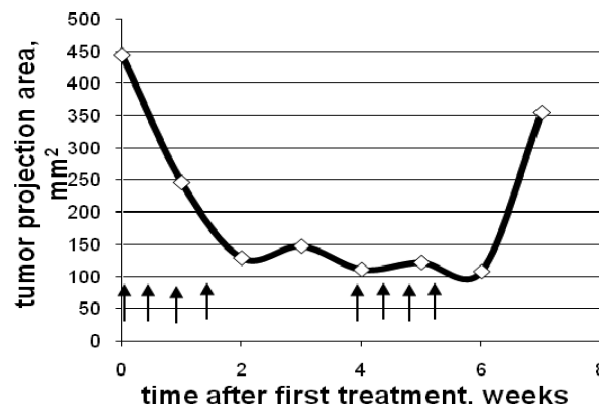

Figure 5. Growth/regression curve of a large pancreatic tumor treated with the combination drug GEM + nbGEN combined with tumor sonication by continuous wave 1 MHz ultrasound applied for 30 s at 3.4 W/cm^2 nominal power density to the mouse abdominal area in the pancreas region. Arrows indicate days of treatment.
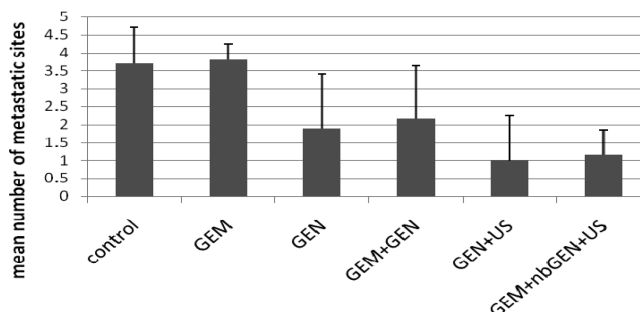

Figure 6. Suppression of metastasis by the ultrasound-mediated chemotherapy of pancreatic cancer using micellar or nanodroplet encapsulated paclitaxel ($N = 6$).

sion of ascites formation (Figure 6). Ascites was clearly visible in ultrasound images of control or GEM-treated tumors (Figure 7); no ascites was found in images of ultrasound-treated tumors or postmortem. This important effect was unexpected and counterintuitive. Possible reasons of metastasis suppression are discussed below.

Note that, for all treatment groups, treatment interruption for two weeks after the first treatment round resulted in tumor regrowth. A second treatment with the same regimen was less effective than the first one.[4] In the Genexol PM and GEM + Genexol PM groups, residual tumors stabilized but
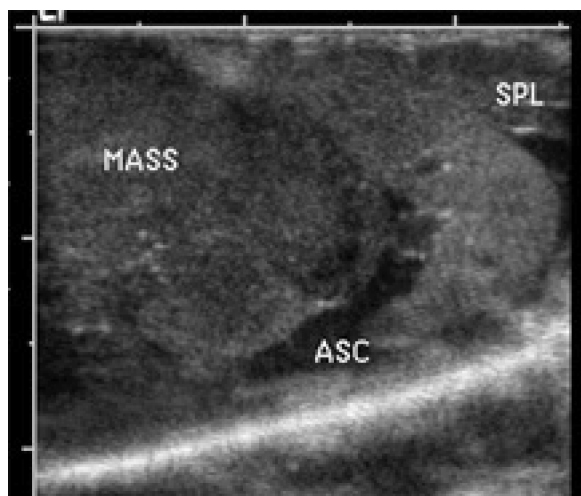
Figure 7. Ultrasound image of the control pancreatic tumor. MASS, tumor; ASC, ascites; SPL, spleen.
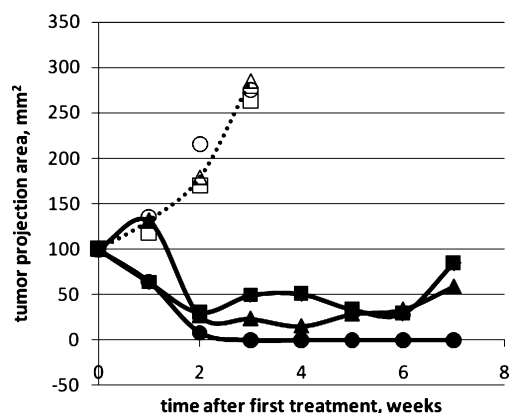
Figure 8. Tumor growth curves for mice treated by GEM (open symbols) or nbGEN + GEM + ultrasound (closed symbols). Different symbols correspond to different animals. Intragroup variation is larger for a nanodroplet encapsulated drug than for a molecularly dissolved drug.

did not regress during the second treatment round; only nanodroplet/ultrasound therapy resulted in some regression of regrown tumors during the second treatment round. This data suggest that either some resistance to paclitaxel developed in the course of the initial treatment or resistant cells were selected during the first treatment round.

With any treatment protocol, local tumor recurrence was observed after completion of treatment. The local recurrence occurred even when the residual tumor could not be resolved by RFP imaging. The possible reasons for this effect are discussed below.

It is noteworthy that the intragroup variations were larger for micellar or nanodroplet encapsulated paclitaxel groups than for control or GEM group. An example for GEM and nbGEN + GEM + ultrasound group is shown in Figure 8.

Discussion

Experimental results are briefly summarized below.

Gemcitabin Resistance and PTX Sensitivity. The tumor growth curve for GEM was very close to that for a control

group, confirming GEM resistance of MiaPaCa-2 cells reported earlier in ref 58. In this work, the GEM resistance of MiaPaCa-2 cells was ascribed to the action of a multidrug resistance associated protein MRP. MRPs are a subfamily of the ATP-binding cassette (ABC) superfamily of transporter proteins. MRPs are separate and distinct from the well-known family of transporter proteins called P-glycoproteins (P-gp). MRPs are usually localized in plasma membranes[59,60] but may be relocated to the intracellular membranes of late endosomes and lysosomes.[61] As indicated by its name, the MRP action is expressed against a plethora of drugs. It was shown in ref 58 that GEM-resistant MiaPaCa-2 cells were sensitive to paclitaxel. This was confirmed in the present study. Animal treatment with micellar encapsulated paclitaxel, Genexol PM resulted in a substantial tumor regression (Figure 4). Cell culture experiments showed that MiaPaCa-2 cells were sensitive to dissolved paclitaxel, Taxol, as well as micellar paclitaxel Genexol PM (data not shown). These data indicate that GEM resistance of MiaPaCa-2 cells is not a multidrug resistance and is not caused by the action of plasma membrane pumps that would have acted on both paclitaxel and GEM.

GEM and paclitaxel have profoundly different mechanisms of action. GEM is the nucleoside analogue, and its site of action is in cell nuclei. On the contrary, paclitaxel acts by stabilizing microtubules in cytoplasm thus mechanically preventing cell division. The sensitivity of GEM-resistant MiaPaCa-2 cells to Genexol PM suggests that paclitaxel loaded in PEG-PLLA micelles successfully overcomes plasma membrane barriers thus allowing paclitaxel interaction with microtubules. GEM resistance of MiaPaCa-2 cells may be caused by the action of nuclear pumps that exert no effect on paclitaxel. Other possible mechanisms include several genetic and/or epigenetic alterations; the latter include gene products associated with gemcitabine transport and metabolism (for a recent review, see ref 62).

(58) Kim, S. O.; Lee, S. W.; Jeong, S. W.; Jung, Y. A.; Kang, S. Y.; Kumar, S.; Oh, H. S. Superior antitumor efficacy of Genexol-PM®, a biodegradable polymeric micelle-based formulation of paclitaxel (Genexol®) compared with Gemzar® (gemcitabine) and Taxol® in human pancreatic cancer cells in vitro and in vivo. Experimental and Molecular Therapeutics 10: Drug Targeting. *Proc. Am. Assoc. Cancer Res.* **2005**, *46*, Abstract 1440.

(59) Barrand, M. A.; Robertson, K. J.; Neo, S. Y.; Rhodes, T.; Wright, K. A.; Twentyman, P. R.; Scheper, R. J. Localisation of the multidrug resistance-associated protein, MRP, in resistant large-cell lung tumour cells. *Biochem. Pharmacol.* **1995**, *50* (10), 1725–9.

(60) Brechot, J. M.; Hurbain, I.; Fajac, A.; Daty, N.; Bernaudin, J. F. Different pattern of MRP localization in ciliated and basal cells from human bronchial epithelium. *J. Histochem. Cytochem.* **1998**, *46* (4), 513–7.

(61) van den Bout, I.; van Rheenen, J.; van Angelen, A.; de Rooij, J.; Wilhelmsen, K.; Jalink, K.; Divecha, N.; Sonnenberg, A. Investigation into the mechanism regulating MRP localization. *Exp. Cell Res.* **2008**, *314* (2), 330–341.

(62) Kim, M. P.; Gallick, G. E. Gemcitabine resistance in pancreatic cancer: picking the key players. *Clin. Cancer Res.* **2008**, *14* (5), 1284–5.

Low effecacy of GEM has warranted studies of combination drugs.[63−65] Therefore in this study, we included GEM as a component of a combination formulation with Genexol PM. It was found that combination treatment by GEM + Genexol PM was slightly more effective than Genexol PM alone though the main effect was undoubtedly exerted by Genexol PM (in a paired *T* test, statistically significant differences were manifested between these groups, $P = 0.01$) (Figure 4). This suggests that Genexol PM may affect intracellular mechanisms involved in GEM inactivation, which deserves further exploration.

Ultrasound Effects. The most efficient tumor regression was observed during systemic treatment with nanodroplet encapsulated paclitaxel combined with tumor-directed ultrasound. As suggested by ultrasound imaging, nanodroplets with encapsulated paclitaxel accumulated in tumor tissue. They converted into microbubbles and released their drug load under the action of tumor-directed ultrasound, which resulted in efficient chemotherapy of pancreatic cancer. However, local tumor recurrence was observed during the treatment break or after the completion of treatment and the recurrent tumors proved more resistant to the same treatment regimen, indicating developed drug resistance or selection for the resistant cells during the initial treatment. A possible reason for this adverse effect is discussed below.

Tumor Recurrence. Ultrasound imaging manifested a highly nonuniform distribution of nanodroplets throughout the tumor volume (Figure 9). This may be caused by the irregularity in tumor vascularization and distribution of interendothelial gaps, which may result in intragroup variability. Doppler images showed the blood vessels that could be resolved by the instrument (hundreds of micrometer size) localized at the tumor periphery or around the tumor (Figure 10); smaller capillaries could not be resolved, but tumors are known to have irregular vascularization.[7,8]

After drug release, irregularity of nanoparticle extravasation would result in drug gradients within the tumor volume. If this is the case, some tumor sites may be exposed to subtherapeutic concentrations of drug, which would favor development of drug resistance. This problem may be solved,
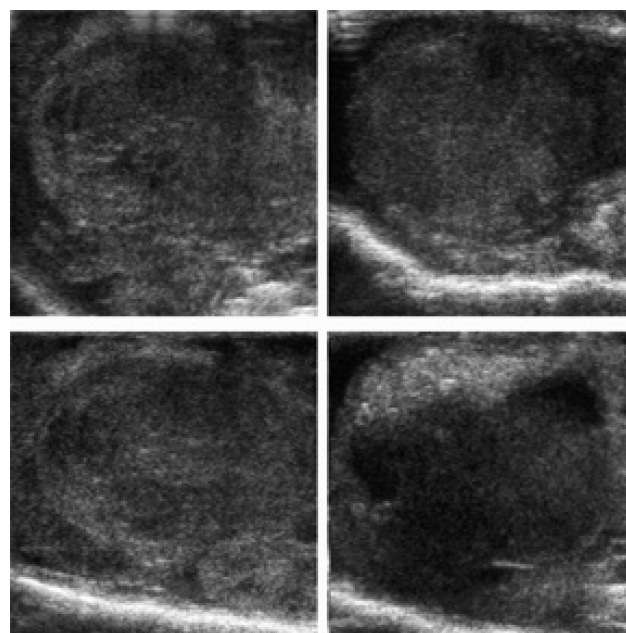
Figure 9. Grayscale distribution in four slices of the same tumor recorded 5 h after the systemic injection of the nanodroplet encapsulated paclitaxel (nbGEN).
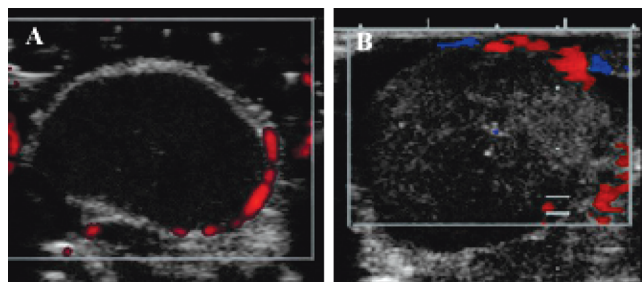
Figure 10. Power Doppler image of the subcutaneous control pancreatic tumor (A) and color Doppler image of the orthotopic pancreatic tumor recorded 5 h after the systemic injection of the nanodroplet encapsulated paclitaxel (B). Vascularization is visible at the periphery or around the tumor. The increase in tumor echogenicity manifests the nanodroplet accumulation.

at least partly, by tumor sonication. Ultrasound is known to enhance diffusion.[66,67] In our earlier work with micellar doxorubicin we found that the intratumoral drug distribution was significantly more uniform in sonicated tumors.[6] However, the degree of drug equalization would depend on the mechanical properties of tumor tissue and tumor vascularization. The above problem may be pertinent to any nanoparticle-associated drug delivery modality. In order to suppress or prevent the development of drug resistance, introduction of MDR-suppressing agents into nanoparticle drug formulations may be warranted.

(63) van Moorsel, C. J.; Pinedo, H. M.; Veerman, G.; Guechev, A.; Smid, K.; Loves, W. J.; Vermorken, J. B.; Postmus, P. E.; Peters, G. J. Combination chemotherapy studies with gemcitabine and etoposide in non-small cell lung and ovarian cancer cell lines. *Biochem. Pharmacol.* **1999**, *57* (4), 407–15.

(64) Crino, L.; Scagliotti, G.; Marangolo, M.; Figoli, F.; Clerici, M.; De Marinis, F.; Salvati, F.; Cruciani, G.; Dogliotti, L.; Pucci, F.; Paccagnella, A.; Adamo, V.; Altavilla, G.; Incoronato, P.; Trippetti, M.; Mosconi, A. M.; Santucci, A.; Sorbolini, S.; Oliva, C.; Tonato, M. Cisplatin-gemcitabine combination in advanced non-small-cell lung cancer: a phase II study. *J. Clin. Oncol.* **1997**, *15* (1), 297–303.

(65) Berlin, J. D.; Catalano, P.; Thomas, J. P.; Kugler, J. W.; Haller, D. G.; Benson, A. B., 3rd. Phase III study of gemcitabine in combination with fluorouracil versus gemcitabine alone in patients with advanced pancreatic carcinoma: Eastern Cooperative Oncology Group Trial E2297. *J. Clin. Oncol.* **2002**, *20* (15), 3270–5.

(66) Lenart, I.; Auslander, D. The effect of ultrasound on diffusion through membranes. *Ultrasonics* **1980**, *18* (5), 216–8.

(67) Mitragotri, S. Effect of therapeutic ultrasound on partition and diffusion coefficients in human stratum corneum. *J. Controlled Release* **2001**, *71* (1), 23–9.

Another intriguing effect that deserves exploration is related to the suppression of pancreatic tumor metastases by ultrasound-mediated chemotherapy with micellar- or nanoemulsion encapsulated paclitaxel (Figure 6). Recent works have revealed that mechanical forces can profoundly influence cell behavior by affecting cell spread, growth, survival and motility. For instance, it was shown that tumors in the pancreas display compromised laminin and type IV collagen basement membrane organization and thinning that, when combined with outward projecting compression force, facilitates tumor cell invasion into the parenchyma.[68] Research on the mechanical components of tumor growth, survival and motility is still in its infancy.[68−70] A better understanding of how mechanical force signals regulate tumor progression and metastasis could significantly accelerate the development of improved treatments.

Transmembrane integrins are the most likely mechano transducers. Two families of proteins are currently implicated in this function: Rho (a member of the Ras protein superfamily)[71,72] and PINCH.[73] The latter functions as an adapter at a key convergence point for integrin and growth factor signal transduction. It was shown that PINCH is upregulated in the stroma of common cancers, notably at invasive edges. This seems important, as the dense desmoplastic infiltration within the tumor is a unique characteristic of PDA. Since PINCH has been shown to play a role in cell migration and signal transduction, PINCH expression may serve a potential marker for tumor invasion. Research on animal models and pancreatic human tissue revealed that PINCH expression is associated with a more aggressive pancreatic tumor and shorter survival.[57] We hypothesize that reduction of metastases in animals treated by Genexol PM or nbGEN and ultrasound may be associated with a concomitant reduction of PINCH expression due to the ultrasound effect on cell membranes. These experiments are currently in progress.

In conclusion, for effective PDA therapy, paclitaxel delivery in PFP nanoemulsions may be combined with endoscopic, extracorporeal, or even intraductal ultrasound applicators. Our experiments demonstrated that low-power output application of ultrasound was able to release the drug into tumor tissue.[2−4] Experimental intraductal transducers are being developed in France; these would allow the most precise tumor sonication. A substantial reduction of the required ultrasonic energy would solve a number of difficult technological problems for the intraductal application. Recent advances in focusing extracorporeal ultrasound on the pancreas[74] suggests that this approach to pancreatic sonication may also become available clinically in the near future.

Conclusions

Ultrasound-mediated therapy with the combination drug formulation GEM + nanodroplet-encapsulated paclitaxel nbGEN combined with tumor sonication with 1 MHz ultrasound exerted a strong therapeutic effect and produced dramatic regression of even very large PDA tumors. Ultrasound-mediated therapy resulted in suppression of metastases and ascites, suggesting improved control of invasive cancer cells. Tumor relapse was observed after the completion of therapy, and recurrent tumors proved more resistant to the same therapy, indicating development of resistance, which may be caused by drug gradients in tumor volume and presence of zones with subtherapeutic drug concentration. This problem may be pertinent to any therapy that relies on nanoparticle extravasation and may require the addition of MDR suppressing agents into nanoparticle drug formulations.

Supporting Information Available: Table 1 presenting particle size distribution parameters for empty and PTX-loaded PEG-PLLA micelles and nanodroplets. AVI video file showing scanned ultrasound images of a pancreatic tumor taken 5 h after the systemic injection of PTX-loaded PEG-PLLA nanodroplets. This material is available free of charge via the Internet at http://pubs.acs.org.

MP900128X

(68) Erler, J. T.; Weaver, V. M. Three-dimensional context regulation of metastasis. *Clin. Exp. Metastasis* **2009**, *26* (1), 35–49.

(69) Cretu, A.; Brooks, P. C. Impact of the non-cellular tumor microenvironment on metastasis: potential therapeutic and imaging opportunities. *J. Cell. Physiol.* **2007**, *213* (2), 391–402.

(70) Butcher, D. T.; Alliston, T.; Weaver, V. M. A tense situation: forcing tumour progression. *Nat. Rev. Cancer* **2009**, *9* (2), 108–22.

(71) Huang, S.; Ingber, D. E. Cell tension, matrix mechanics, and cancer development. *Cancer Cell* **2005**, *8* (3), 175–6.

(72) Paszek, M. J.; Zahir, N.; Johnson, K. R.; Lakins, J. N.; Rozenberg, G. I.; Gefen, A.; Reinhart-King, C. A.; Margulies, S. S.; Dembo, M.; Boettiger, D.; Hammer, D. A.; Weaver, V. M. Tensional homeostasis and the malignant phenotype. *Cancer Cell* **2005**, *8* (3), 241–54.

(73) Wang-Rodriguez, J.; Dreilinger, A. D.; Alsharabi, G. M.; Rearden, A. The signaling adapter protein PINCH is up-regulated in the stroma of common cancers, notably at invasive edges. *Cancer* **2002**, *95* (6), 1387–95.

(74) Hwang, J. H.; Wang, Y. N.; Warren, C; Upton, M. P.; Starr, F.; Zhou, Y.; Mitchell, S. B. Preclinical in vivo evaluation of an extracorporeal HIFU device for ablation of pancreatic tumors. *Ultrasound Med. Biol.* **2009**, *35* (6), 967–75.